Design of Optical Circuit Devices Using Topology Optimization Method With Function-Expansion-Based Refractive Index Distribution

Yasuhide Tsuji, *Member, IEEE*, and Koichi Hirayama, *Senior Member, IEEE*

***Abstract*—We propose a design method for optical waveguide devices based on topology optimization with alternative expression of refractive index distribution. In our approach, a refractive index distribution in a design region is expressed by an expansion with some analytical functions and gray area, which has intermediate refractive index between usable materials, does not appear. We can obtain better results in the optimization of waveguide bends and branches, compared with the widely used density method.**

***Index Terms*—Finite-element method, optical circuit device, topology optimization.**

I. Introduction

In THE recent progress of optical communication systems, many kinds of high-performance optical waveguide devices have been developed. Especially, photonic crystal waveguides and silicon nanophotonic waveguides have great possibility to improve device performance and compactness of photonic circuits and extensive researches on those waveguides are being carried out.

In order to improve device performance of such high index contrast waveguides, the design theory based on weakly guiding [1] is not likely to be often used and the development of optimization technique is highly expected. Recently, in order to find the optimum structure of photonic and microwave circuits, topology optimization method begins to be used [2]–[14]. The topology optimization method is a class of optimization methods that can simultaneously deal not only with geometric form but also with topological configuration, so we can find out optimized structures without predefining any geometry. In general, the density method is used to express refractive index distribution. However, in the topology optimization method with the widely used density method, since the density parameters are continuous, those values can be intermediate values between 0 and 1. This corresponds to an intermediate value between the refractive indexes of usable materials and is not desirable. To suppress these gray areas which have intermediate value of refractive index, the method based on imaginary conductivity has been proposed and can improve optimized structure [8], but it cannot completely eliminate gray areas. As an alternative approach, a geometry projection method has been reported [15]. In this method, through the optimization process, material boundaries are distinctly defined and are allowed to move, merge, and disappear, but the new boundaries cannot be created.

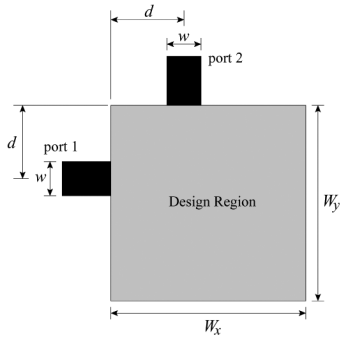

Fig. 1. Design structure for 90° bend.

In this letter, we propose a topology optimization method with alternative expression for refractive index distributions. In this approach, the refractive index distribution is determined by a projection of some continuous function, which is expressed by the form of function expansion with primitive basis functions and the amplitude parameters of the basis functions are optimized according to the sensitivity analysis. In this approach, the material boundaries are distinctly defined and no gray area appears in the design region. Moreover, any initial structure in the design region is not required.

As numerical examples, we demonstrate how the method can be used for 90° bends and 1 : 1 T-branching waveguides and compare the results obtained by the present method and those by the topology optimization with the density method.

II. Expression for Refractive Index Distribution in Topology Optimization Method

As an example, we consider a waveguide bend as shown in Fig. 1 and maximize the transmission power into the output port 2 using the topology optimization method based on the finite-element method with a perfectly matched layer [16].

Using the widely used density method for the expression of refractive index distribution, the permittivity in each element within the design region is expressed as follows:

$$\varepsilon_{rj} = \varepsilon_{ra} + (\varepsilon_{rb} - \varepsilon_{ra})\rho_j^p, \qquad (0 \le \rho_j \le 1) \qquad (1)$$

where j denotes the element number in the finite-element mesh, ε_{ra} and ε_{rb} are the relative permittivities of two usable material, respectively, ρ_j is the density parameter in the jth element, p is the penalization parameter used to suppress gray areas, in which the relative permittivity has the intermediate value between two

Manuscript received December 28, 2007; revised March 16, 2008.

The authors are with the Department of Electrical and Electronic Engineering, Kitami Institute of Technology, Kitami 090-8507, Japan (e-mail: tsujiya@mail.kitami-it.ac.jp; hirakc@mail.kitami-it.ac.jp).

Color versions of one or more of the figures in this letter are available online at http://ieeexplore.ieee.org.

Digital Object Identifier 10.1109/LPT.2008.922921

usable values. Through an iteration process, according to the sensitivity analysis, the density parameters are optimized to improve the objective function. However, in the most cases, some of the density parameters have intermediate values between 0 and 1 and material boundaries cannot be distinctly defined.

In this letter, we propose an expression of refractive index distribution based on a function expansion as follows:

$$\varepsilon_r(x,y) = \varepsilon_{ra} + (\varepsilon_{rb} - \varepsilon_{ra})\, H(\varphi(x,y))$$
$$H(z) = \begin{cases} 0, & (z \le -h) \\ 0.5\left(\frac{z}{h+1}\right)^2, & (-h < z \le 0) \\ 1 - 0.5\left(\frac{z}{h-1}\right)^2, & (0 < z < h) \\ 1, & (z \ge h) \end{cases} \tag{2}$$

where $\varphi(x,y)$ is some function used to determine the refractive index distribution. The function $H(z)$ is used to convert the value of $\varphi(x,y)$ into the one of the relative permittivities of two usable materials. In order to make it possible to take differential of $H(z)$ in the sensitivity analysis; $H(z)$ has a transient region of width $2h$. In this letter, h is set to be 0.02 for the sensitivity analysis and 0 for the optimized structure. In the following calculations, there was little difference between the results for $h = 0$ and $h = 0.02$. $\varphi(x,y)$ is normalized so that its maximum value may become one. Although several kinds of expressions for $\varphi(x,y)$ are available, in this letter, we employ following sinusoidal-function-based expression:

$$\varphi(x,y) = \sum_{i=-N_x}^{N_x} \sum_{j=-N_y}^{N_y} (a_{ij}\cos\theta_{ij} + b_{ij}\sin\theta_{ij})$$
$$\theta_{ij} = \frac{2\pi i}{L_x}x + \frac{2\pi j}{L_y}y$$

where $2N_x + 1$, $2N_y + 1$ are numbers of expansion functions along the x and y directions. L_x and L_y are set to be greater than W_x and W_y, respectively. The partial differential of relative permittivity with respect to a_{ij} or b_{ij} required in the sensitivity analysis can be easily calculated as follows:

$$\frac{\partial \varepsilon_r}{\partial a_{ij}} = \cos\theta_{ij} f(\varphi(x,y))$$
$$\frac{\partial \varepsilon_r}{\partial b_{ij}} = \sin\theta_{ij} f(\varphi(x,y))$$
$$f(z) = \begin{cases} \frac{(z+h)}{h^2}, & (-h < z \le 0) \\ \frac{(h-z)}{h}^2, & (0 < z < h) \\ 0, & (|z| \ge h). \end{cases}$$

In the density method, through the iteration process, the refractive index in each element is gradually updated toward the one of the usable values. On the other hand, in the present approach, the shape of the boundaries between two usable materials is updated.

III. Numerical Examples

As numerical examples of the present design method, first, we consider the 90° bend as shown in Fig. 1, which is the same example in [10]. The refractive indexes of cladding and core are $n_a = 1.0$ and $n_b = 1.45$, respectively. The waveguide width is $w = 0.7$ μm, the design region widths are $W_x = 4$ μm and $W_y = 4$ μm, respectively, $d = 1.5$ μm, $N_x = N_y = 8$, and $L_x = L_y = 6$ μm. The size of each element is 0.05 μm. We assume that the fundamental TE mode with wavelength $\lambda = 1.55$ μm is launched into port 1. Fig. 2 shows the optimized refractive index distribution and electric field intensity. As an initial condition for amplitude parameters, we set a_{00} to be -0.01 and the others to be 0. The sequential linear programming is employed to optimize the parameters, a_{ij} and b_{ij}. The normalized transmission power into output port 2 is 0.96. This result is slightly better than that in [10] and material boundary is clearly defined. Fig. 3 shows the convergence behavior of the transmission powers until 20 iteration steps. The convergence property is also improved in this problem compared with that in [10]. We think that this is because the numbers of optimized parameters in our approach are less than that in the density method and the first iteration process provided similar structure to the final optimized one by chance. However, in order to express fine structures, more expansion functions may be needed and more detailed discussion about the convergence behavior has to be studied. Fig. 4 shows the obtained function $\varphi(x,y)$ and projected refractive index distribution.

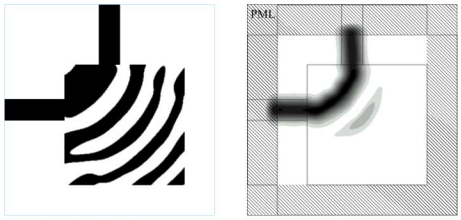

Fig. 2. Optimized 90° bend by topology optimization. (a) Refractive index distribution; (b) field intensity.

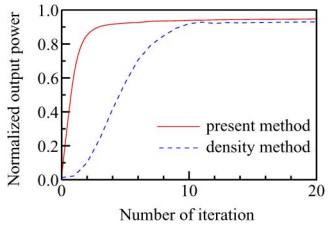

Fig. 3. Convergence behavior of normalized output power.

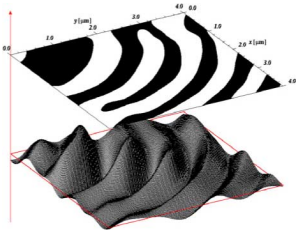

Fig. 4. Optimized $\varphi(x,y)$ and projected refractive index distribution.

Next, we consider the same example of T-branching waveguide in [10], as shown in Fig. 5. The design region widths are $W_x = 4$ μm and $W_y = 3$ μm, respectively, and the other parameters are the same as in the case of 90° bend. In this example, considering 1 : 1 branching, we use the symmetric condition along the y direction and maximize the transmission power into

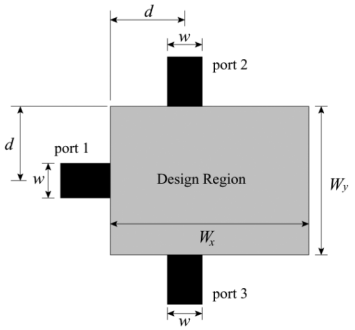

Fig. 5. Design structure for T-branching waveguide.

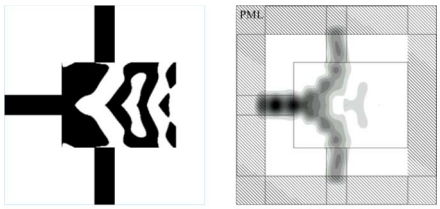

Fig. 6. Optimized T-branching waveguide by topology optimization. (a) Refractive index distribution; (b) field intensity.

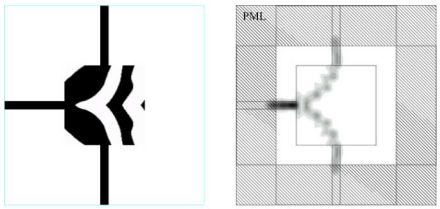

Fig. 7. Optimized T-branching waveguide with higher refractive index contrast by topology optimization. (a) Refractive index distribution; (b) field intensity.

each output port. Fig. 6 shows the optimized refractive index distribution and electric field intensity. The normalized transmission powers into output ports 2 and 3 are 0.46, respectively, and these are the almost same as those in [10]. The optimized structure in [10] is a little bit complicated and has a relatively large gray area. On the other hand, the refractive index distribution obtained here has no gray area and has a relatively simpler structure than that in [10].

Finally, we consider a $1:1$ T-branching waveguide with higher refractive index contrast between core and cladding. Here, the cladding and core refractive indexes are assumed to be 1.0 and 3.2, respectively. The structural parameters are $w = 0.2$, $W_x = W_y = 2\ \mu$m, and $L_x = L_y = 3.5\ \mu$m. The fundamental TE mode with wavelength $\lambda = 1.55\ \mu$m is launched into port 1. Fig. 7 shows the optimized refractive index distribution and electric field intensity. The normalized transmission powers into output ports 2 and 3 are 0.49, respectively. In the optimized structure, there is a wedge-shaped indent between the design region and the exit ports. We think this is caused by the selection of the expansion function and has no physical meaning.

IV. Conclusion

We proposed a topology optimization method with function-expansion-based refractive index distribution. Compared with the density method, in the present approach, no gray area appears in the optimized refractive index distribution and material boundaries are distinctly defined. In this approach, the optimized structure can be controlled by selection of the expansion function to some degree and other kinds of functions can be also available. Extending this method to three-dimensional structures is now under consideration.

References

[1] Y. Sakamaki, T. Saida, T. Shibata, Y. Hida, T. Hashimoto, M. Tamura, and H. Takahashi, "Y-branch waveguides with stabilized splitting ratio designed by wavefront matching method," *IEEE Photon. Technol. Lett.*, vol. 18, no. 7, pp. 817–819, Apr. 1, 2006.

[2] G. Kiziltas, D. Psychoudakis, J. L. Volakis, and N. Kikuchi, "Topology design optimization of dielectric substrates for bandwidth improvement of a patch antenna," *IEEE Trans. Antennas Propag.*, vol. 51, no. 10, pp. 2732–2743, Oct. 2003.

[3] J. S. Jensen and O. Sigmund, "Systematic design of photonic crystal structures using topology optimization: Low-Loss waveguide bends," *Appl. Phys. Lett.*, vol. 84, no. 12, pp. 2022–2024, Mar. 2004.

[4] P. I. Borel, A. Harpøth, L. H. Frandsen, M. Kristensen, P. Shi, J. S. Jensen, and O. Sigmund, "Topology optimization and fabrication of photonic crystal structures," *Opt. Express*, vol. 12, no. 9, pp. 1996–2001, May 2004.

[5] L. H. Frandsen, A. Harpøth, P. I. Borel, M. Kristensen, J. S. Jensen, and O. Sigmund, "Broadband photonic crystal waveguide 60° bend obtained utilizing topology optimization," *Opt. Express*, vol. 12, no. 24, pp. 5916–5921, Nov. 2004.

[6] W. R. Frei, D. A. Tortorelli, and H. T. Johnson, "Topology optimization of a photonic crystal waveguide termination to maximize directional emission," *Appl. Phys. Lett.*, vol. 86, no. 11, Mar. 2005, Article 111114.

[7] J. S. Jensen, O. Sigmund, L. H. Frandsen, P. I. Borel, A. Harpøth, and M. Kristensen, "Topology design and fabrication of an efficient double 90° photonic crystal waveguide bend," *IEEE Photon. Technol. Lett.*, vol. 17, no. 6, pp. 1202–1204, Jun. 2005.

[8] J. S. Jensen and O. Sigmund, "Topology optimization of photonic crystal structures: A high bandwidth low-loss T-junction waveguide," *J. Opt. Soc. Amer. B, Opt. Phys.*, vol. 22, no. 6, pp. 1191–1198, Jun. 2005.

[9] A. Têtu, M. Kristensen, L. H. Frandsen, A. Harpøth, P. I. Borel, J. S. Jensen, and O. Sigmund, "Broadband topology-optimized photonic crystal components for both TE and TM polarizations," *Opt. Express*, vol. 13, no. 21, pp. 8606–8611, Oct. 2005.

[10] Y. Tsuji, K. Hirayama, T. Nomura, K. Sato, and S. Nishiwaki, "Design of optical circuit devices based on topology optimization," *IEEE Photon. Technol. Lett.*, vol. 18, no. 7, pp. 850–852, Apr. 1, 2006.

[11] Y. Watanbe, Y. Sugimoto, N. Ikeda, N. Ozaki, A. Mizutani, Y. Takata, Y. Kitagawa, and K. Asakawa, "Broadband waveguide intersection with low crosstalk in two-dimensional photonic crystal circuits by using topology optimization," *Opt. Express*, vol. 14, no. 20, pp. 9502–9057, Oct. 2006.

[12] Y. Watanabe, N. Ikeda, Y. Sugimoto, Y. Takata, Y. Kitagawa, A. Mizutani, N. Ozaki, and K. Asakawa, "Topology optimization of waveguide bends with wide, flat bandwidth in air-bridge-type photonic crystal slabs," *J. Appl. Phys.*, vol. 101, no. 11, Jun. 2007, Article 113108.

[13] K. Hirayama, Y. Tsuji, T. Nomura, K. Sato, and S. Nishiwaki, "Application of topology optimization to H-plane waveguide component," *IEICE Trans. Electron.*, vol. E90-C, no. 2, pp. 282–287, Feb. 2007.

[14] J. Riishede and O. Sigmund, "Inverse design of dispersion compensating optical fiber using topology optimization," *J. Opt. Soc. Amer. B, Opt. Phys.*, vol. 25, no. 1, pp. 88–97, Jan. 2008.

[15] W. R. Frei, D. A. Totorelli, and H. T. Johnson, "Geometry projection method for optimizing photonic nanostructures," *Opt. Lett.*, vol. 32, no. 1, pp. 77–79, Jan. 2007.

[16] Y. Tsuji and M. Koshiba, "Finite element method using port truncation by perfectly matched layer boundary conditions for optical waveguide discontinuity problems," *J. Lightw. Technol.*, vol. 20, no. 3, pp. 463–468, Mar. 2002.